# 1P4-6

# Estimation of Fire Damage Depth of Mortar Using Surface Acoustic Waves Propagation by Non-liner Aerial Ultrasonic Waves

非線形空中超音波による弾性表面波伝搬を利用した
モルタルの火害深さ推定

Takuya Saito[1‡], Ayumu Osumi[1], and Youichi Ito[1] ([1]Coll.Sci. and Tech., Nihon Univ.)
齊藤 卓哉 [1‡], 大隅 歩 [1], 伊藤 洋一 [1] ([1] 日大・理工)

## 1. Introduction

Generally, building materials are damaged at high temperatures resulting from fire. Estimating the decrease in strength or elastic modulus of building materials after fire is an important diagnostic action that determines whether the structure is available and the scale of repair needed.

Here, we aim to show a nondestructive non-contact practical method of diagnosing fire damage [1,2], using high-intensity aerial ultrasonic waves [3] and optical equipment. For example, we have estimated the change in the elastic modulus by examining the vibration velocity distribution of a target surface and the change in the propagation speed of the surface acoustic waves (SAWs) excited by high-intensity aerial ultrasonic waves. An important task in diagnosing fire damage is to estimate the depth of damage to the target.

In this report, as a basic study, we attempt to estimate the depth of fire damage to mortar by examining the change in propagation speeds of SAWs at various frequencies.

## 2. Experimental Method

**Fig. 1** shows an outline of the experimental equipment. The devices include a sound source (driving frequency 26.6 kHz) that can emit high-intensity aerial ultrasonic waves and a laser Doppler vibrometer (LDV) that measures vibration of the surface. A sound wave is focused at a position about 310 mm from the sound source, resulting in a sound pressure of about 5000 Pa (Overall) at the focal point, generated from electric input power of 10 W. In addition, a harmonic of integer multiples of the fundamental frequency (drive frequency) is generated in the radiated sound wave because the sound waves are strongly nonlinear.

In the experiment, the vibration generated at the mortar surface by irradiation with this high-intensity acoustic wave is measured by the LDV, which does not contact the surface. To avoid the influence of high-intensity acoustic waves on LDV

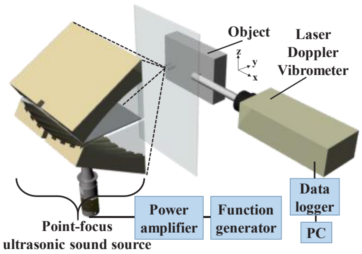


Fig. 1 Schematic view of experiment system

measurement, sound waves are also transmitted to the vicinity of the target by pipes (material: acrylic; inner diameter: 8 mm; length: 30 mm).

The LDV uses a three-axis precision stage for accurate movement and acquires the vibration velocity and phase information simultaneously. The measurement timing is triggered by the rise in voltage signal from the sound source immediately after completing the movement to a measurement point.

From the waveform of the obtained vibration velocity, the fundamental frequency and harmonic components are extracted by a band pass filter (center frequency ± 1 kHz), and the SAW propagation is visualized by using the instantaneous vibration velocity distribution of each identified frequency. The SAW propagation image also includes components of the irradiated ultrasonic waves, so a spatial Fourier transformation and a filtering process are performed on the acquired image to isolate the SAW propagation image. The SAW speed is then calculated using the SAW wavelength obtained from the SAW propagation image.

## 3. Experimental Sample

**Fig. 2** shows the mortar sample used in the experiment (size: 220 × 150 × 50 mm). The measurement area (100 × 30 mm) and a point excited by the sound waves being irradiated are showed in the figure. Measurements are made at 1 mm intervals. The sample is covered with a refractory cloth (excluding the surface to be measured) and then heated in an electric furnace (temperature: 850 °C). Thermocouples are embedded at 4 mm, 8 mm, 12

---

Email:osumi.ayumu@nihon-u.ac.jp

mm, and 16 mm from the surface of the burning surface to monitor temperature.

Samples A-C were prepared for different burning times. After burning, each sample was removed from the furnace and allowed to cool naturally to room temperature. **Fig. 3** shows a time series of the temperature inside the sample during burning. With burning time increasing, internal temperatures become higher and it is a possibility that fire damage become deeper.

## 4. Result and Discussion

In the experiment, sound waves were irradiated for 200 cycles of input signal, with 10 W supplied to the sound source, and the vibration waveforms was acquired for 15 ms.

**Fig. 4** shows the SAW propagation image for the second harmonic (53.2 kHz) of sample A every 1/4 cycle. The results confirm SAW propagation. The inter-peak distance at this amplitude is taken as the wavelength of the SAW and the propagation speed of the SAW is calculated. **Table I** shows the propagation speed for each sample (A, B, C) at the second to fourth harmonic frequencies.

From the results, the propagation speed is slow in all samples, corresponding to the length of burning time at the same frequency. Also, the propagation speed is slower for the harmonic vibrations.

We suggest the following explanation. The high-frequency SAWs, having a short wavelength, propagate through a shallower area and are strongly affected by fire damage. For example, the characteristics of sample C shows that the propagation speed tends to approach a constant value as the frequency becomes higher. In fact, the depth of the fire damage can be estimated to some extent from the propagation characteristics.

## 5. Conclusion

We performed an experimental study using noncontact measurement to estimate fire damage in the depth direction of mortar by using high-intensity aerial ultrasonic waves and optical equipment. The results showed measurement of the speed characteristics of the SAW of each frequency for multiple high frequencies generated by high-intensity aerial ultrasonic waves. From the frequency characteristics of the SAW speed, we were able to assess fire damage in the depth direction.

## References

1. A. Osumi and Y. Ito, IEEE. Conf. Publ, 2376 (2010).
2. T. Saito, A. Osumi and Y. Ito, USE2017, 2P2-4 (2017).
3. Y. Ito, Acoust. Sci. Technol 36(3), p. 216-224, (2015).

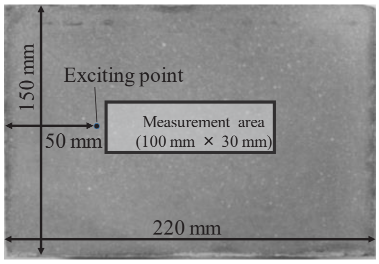


Fig. 2 Experimental Sample

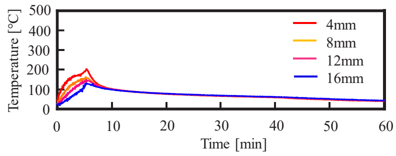


(a) Sample A

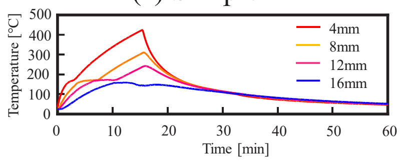


(b) Sample B

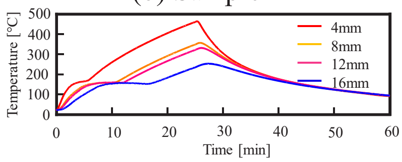


(c) Sample C

Fig. 3 Temperature history at various depths

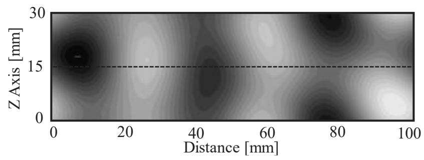


(a) Start of cycle

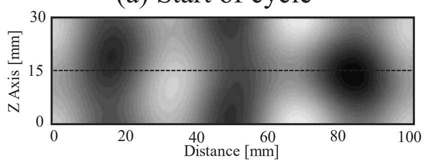


(b) After 1/4 cycle

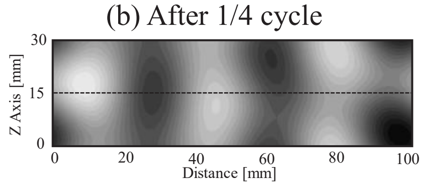


(c) After 1/2 cycle

Fig. 4 Propagation images of sample A (2nd harmonic)

Table I Propagation speed

| | | A | B | C |
|---|---|---|---|---|
| | kHz | m/s | m/s | m/s |
| 2nd | 53.2 | 1800 | 1390 | 1350 |
| 3rd | 79.8 | 1600 | 1280 | 1150 |
| 4th | 106.4 | 1540 | 1200 | 1130 |